Electron Emission Holography at keV Energies: Estimates of Accuracy and Limitations

S. Thevuthasan, G. S. Herman, A. P. Kaduwela, R. S. Saiki, Y. J. Kim, W. Niemczura, M. Burger, and C. S. Fadley[a]

Department of Chemistry, University of Hawaii, Honolulu, Hawaii 96822

(Received 11 January 1991)

We consider the accuracy of holographic inversions of electron emission data at $\sim 10^3$ eV to yield atomic positions. Theoretical calculations for small clusters of 2–5 atoms in both single and multiple scattering show that self-interference effects may be present, and that forward-peaked scattering tends both to shift peaks by as much as 0.5–1.0 Å from the true positions and to elongate images along forward-scattering directions. However, eliminating forward-peaked intensities before inversion significantly improves image quality.

PACS numbers: 61.14.–x, 42.40.Dp, 79.20.Kz

It has recently been suggested by Szoeke [1] and by Barton [2] on theoretical grounds, and then demonstrated in analyses of experimental data for Cu by Tonner and co-workers [3], that the intensity distributions of photoelectrons, Auger electrons, or backscattered Kikuchi electrons above a single-crystal surface can be considered to be holograms, and that such holograms can be inverted using Fourier-transform (FT) methods to yield approximate images of atomic positions. Saldin and de Andres [4] also have used the same FT inversion method in the analysis of experimental diffuse-LEED data. More recent multiple-scattering theoretical modeling of Auger emission from Co overlayers by Wei, Zhao, and Tong [5(a)] also has found features in images associated with some atomic positions. Very recent experimental and theoretical results by Herman *et al.* [6] for Si $2p$ emission from Si(111) also show some features associated with near-neighbor atoms.

Current estimates of the accuracy of such imaging range from ± 0.3 Å to ± 1.0 Å [2–5]. If the central axis of a hologram of full opening angle α is taken to be along the surface normal (i.e., z axis or "vertical" direction) and the electron wavelength is λ_e, then the ideal image resolutions in the limit of s-wave point scattering should be $|\Delta x| = |\Delta y| = 0.61\lambda_e/\sin(\alpha/2)$ in the (x,y) or "horizontal" surface plane, and a larger $|\Delta z| \simeq 2.00\lambda_e/\sin^2(\alpha/2)$ along the vertical direction [2(b)].

The typical electron energies chosen in both theoretical modeling and experiments have so far been in the 500–1000-eV range, as dictated by the need for smaller λ_e's of roughly 0.4–0.5 Å. At these energies, the electron-atom scattering process produces a strong enhancement of intensity in the forward direction, with scattering at angles of more than about 20°–30° being much reduced in strength [7]; such forward-scattering effects provide real-space information on the *directions* of near-neighbor bonds and low-index axes [7]. But little is known about the influence of these anisotropic scattering effects and the scattering phase shifts associated with them, or of more complex multiple-scattering effects, on the images from electron emission holography.

In this Letter, we thus present model calculations for several simple clusters of atoms in an attempt to judge how well electron emission holography can image, and also to assess whether there are methods of data taking or analysis that will reduce the aberrations and/or artifacts present. These calculations have been carried out at both single-scattering (SS) and fully converged multiple-scattering (MS) levels using a recently developed spherical-wave cluster method described elsewhere [8], with the MS results thus being expected to model very well the expected intensity distributions. The electron kinetic energy is 1000 eV. We have assumed an outgoing s wave from the emitter (a common approximation in the simulation of both Auger and Kikuchi diffraction [3,8(b),9]), although we comment briefly below on the effects of using the correct interfering $l \rightarrow l \pm 1$ channels appropriate to photoelectron emission. Unless otherwise noted, Cu scatterers are used, the nearest-neighbor distance in the clusters is that of bulk Cu (2.56 Å), and the hologram opening angle is 178° or very near the full 180° possible.

We first consider a general expression for the intensity distribution expressed as a normalized $\chi(\mathbf{k})$ function [2(a),4,8(a)], where $\mathbf{k}$ is the electron wave vector. If the direct or unscattered component of an outgoing wave from the emitter is denoted by ϕ_0 [with corresponding intensity $I_0(\mathbf{k})$], and the singly, and possibly also multiply, scattered component as it leaves for the detector from the jth scatterer at $\mathbf{r}_j$ is denoted by ϕ_j, then these components can be written very generally as [2(a),8(a)] $\phi_0(\mathbf{r}) = F_0(\mathbf{k})\exp[i\mathbf{k}\cdot\mathbf{r}]$, and $\phi_j(\mathbf{r}) = F_j(\mathbf{k})\exp[i\mathbf{k}\cdot(\mathbf{r}-\mathbf{r}_j)]$; here, $F_0(\mathbf{k})$ contains factors for the excitation matrix elements and inelastic attenuation, and $F_j(\mathbf{k})$ contains these factors as well, but also path-length-dependent phase factors $\exp[ikL_j]$, effective spherical-wave scattering factor(s), Debye-Waller-like factors for vibrational attenuation, and a sum over the various single- and multiple-scattering pathways with different total lengths L_j that terminate in scatterer j just before going to the detector. Summing the direct wave and the scattered waves from all atoms j in a cluster, taking the square to get the intensity $I(\mathbf{k})$, and then determining

$\chi(\mathbf{k})$ from $[I(\mathbf{k})-I_0(\mathbf{k})]/I_0(\mathbf{k})^{1/2}$ yields

$$\chi(\mathbf{k}) \propto \sum_j \{F_0^*(\mathbf{k})F_j(\mathbf{k})\exp[-i\mathbf{k}\cdot\mathbf{r}_j]+F_0(\mathbf{k})F_j^*(\mathbf{k})\exp[i\mathbf{k}\cdot\mathbf{r}_j]\} + \sum_j\sum_k \{F_j^*(\mathbf{k})F_k(\mathbf{k})\exp[i\mathbf{k}\cdot(\mathbf{r}_j-\mathbf{r}_k)]+F_j(\mathbf{k})F_k^*(\mathbf{k})\exp[-i\mathbf{k}\cdot(\mathbf{r}_j-\mathbf{r}_k)]\} . \quad (1)$$

As in prior work, the inversion proceeds by projecting $\chi(\mathbf{k})$ onto the (k_x,k_y) surface plane and then doing a two-dimensional FT to yield the image U in a given z plane as

$$U(x,y;z) \propto \left| \int\int \{\chi(\mathbf{k})\exp[ik_z z]\}\exp[i(k_x x+k_y y)]dk_x\,dk_y \right| . \quad (2)$$

The first (single) sum in Eq. (1) represents the usual hologram of optical holography and the second (double) sum the self-hologram [1,4]. If the F_j's did not depend on $\mathbf{k}$ (implying among other things s-wave scattering), then the FT would be expected to yield peaks only at $\pm\mathbf{r}_j$ [the real and conjugate (twin) images, respectively] and at $\pm(\mathbf{r}_j-\mathbf{r}_k)$ (the images due to self-interference and their conjugates). In the further limit that $|F_0| \gg |F_j|$ for all j, the double sum can be neglected and only the real image and its conjugate will be obtained. However, some $|F_j|$'s are very large, and the dependence of the F_j's on $\mathbf{k}$ is very strong, including both forward-scattering dominance and possible multiple-scattering pathways that introduce additional factors of $\exp[ik|\mathbf{r}_m-\mathbf{r}_n|]$ for each step in a pathway.

Beginning with self-interference effects, we consider a small cluster of five Cu atoms in the shape of a centered hexagon in the (x,y) plane, but with the topmost and bottommost atoms removed [Fig. 1(a)]. The emitter is at the center of the cluster. In order to look for self-interference effects, we have artificially varied the strengths of all scattered waves from $\frac{1}{10}$ to 1 to 10 times their true values by multiplying all F_j's by a variable parameter $\beta=0.1$, 1.0, and 10.0 in the calculations. The resulting contour plots of $U(x,y;0=$in the plane of the cluster) for $\beta=1.0$ and 10.0 are shown in Figs. 1(b) and 1(c), respectively. From the positions of the FT peaks, as well as the scaling of their relative intensities with β (real image $\propto\beta$ and self-image $\propto\beta^2$), we conclude that self-interference effects can indeed be seen, with the peaks labeled a being the real image at $\pm\mathbf{r}_j$ and the peaks labeled b and c being self-interference effects. The self-interference peaks b are abut 18% as strong as the real image peaks a for the true scattering strength in Fig. 1(b). Additional self-interference peaks c are seen as the scattering strength is increased. These results thus indicate that the neglect of self-interference features is only valid as a borderline approximation.

Next we consider the degree to which simple linear chains of Cu atoms with the emitter at one end [8(b),9] can be imaged in both SS and MS simulations. One important MS effect that is found for the energies of interest here is a loss of forward-scattering intensity along the chain due to so-called "defocusing" [10]. We will consider here chains oriented both parallel to a surface, with inelastic attenuation included only along the chain axis, and perpendicular to this surface, with attenuation along all paths below the surface. We will also make reference to idealized SS calculations for which the scattering is forced to give "ideal" holograms by being weak s wave only; this is done by using only the $l=0$ partial wave, with $\beta=1.0$ or less.

In Fig. 2, we show FT results for a horizontal chain containing five atoms as calculated in several approximations. First, the ideal s-wave FT in Fig. 2(a) yields narrow peaks at very near the exact positions of all of the atoms (to within $\sim\pm0.04$–0.08 Å). The full widths at half maximum intensity (FWHM's) of these peaks of ~0.50 Å are furthermore in good agreement with the above-quoted formula for horizontal resolution. In Fig. 2(b), we show results from a single-scattering calculation with full forward-peaked electron-atom scattering (all

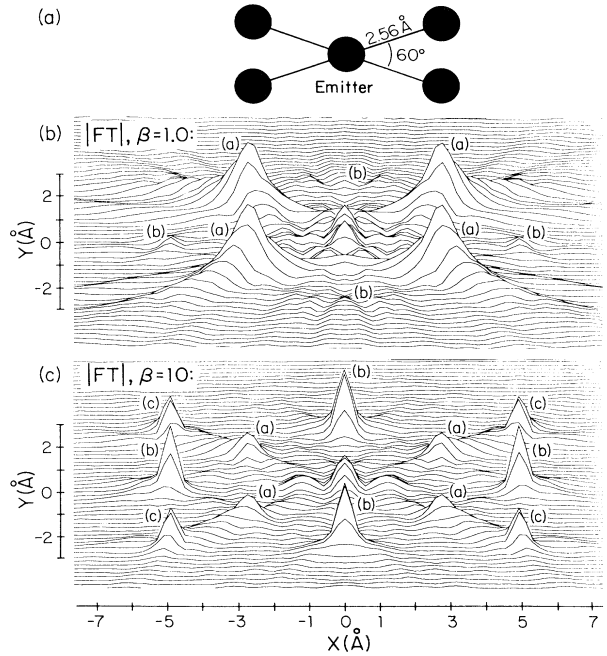

FIG. 1. (a) The geometry of a five-atom cluster in the horizontal (x,y) plane. (b),(c) Horizontal contour stack plots of the in-plane ($z=0.0$ Å) FT's for choices of scattering weight of $\beta=1.0$ (true weight) and 10.0, respectively. a denotes real image peaks and b,c denote self-interference peaks.

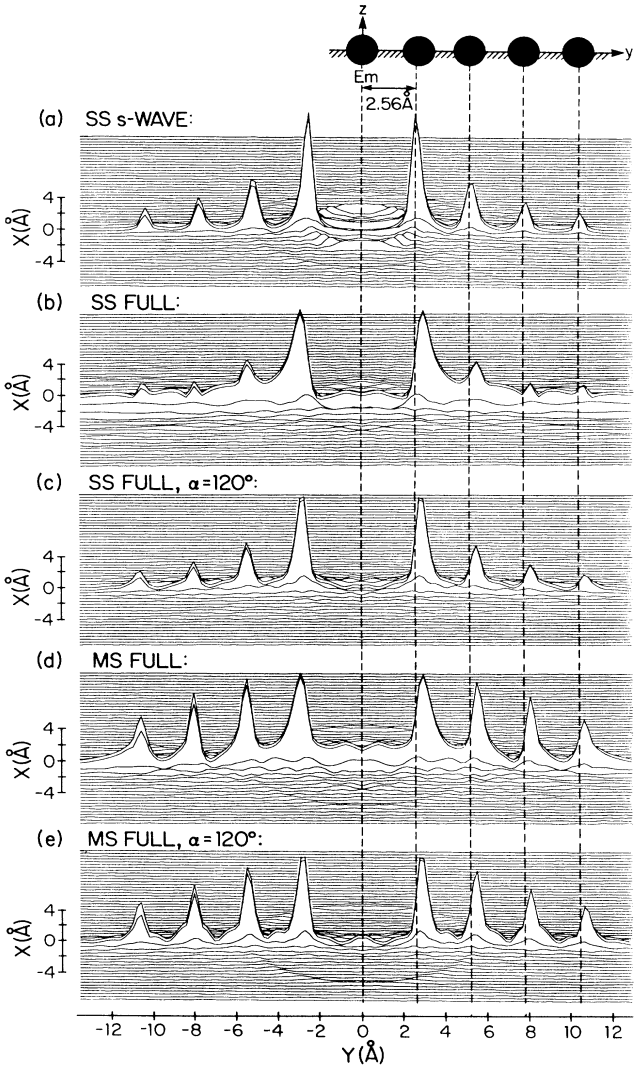

FIG. 2. Horizontal contour plots of the in-plane ($z=0.0$ Å) FT's for s emission from a five-atom horizontal Cu chain. Dashed lines indicate true atomic positions. (a) Ideal weak s-wave single scattering (SS); $\alpha=178°$. (b) Full scattering strength in SS; $\alpha=178°$. (c) As (b), but for $\alpha=120°$. (d) Full scattering strength in MS; $\alpha=178°$. (e) As (d), but for $\alpha=120°$.

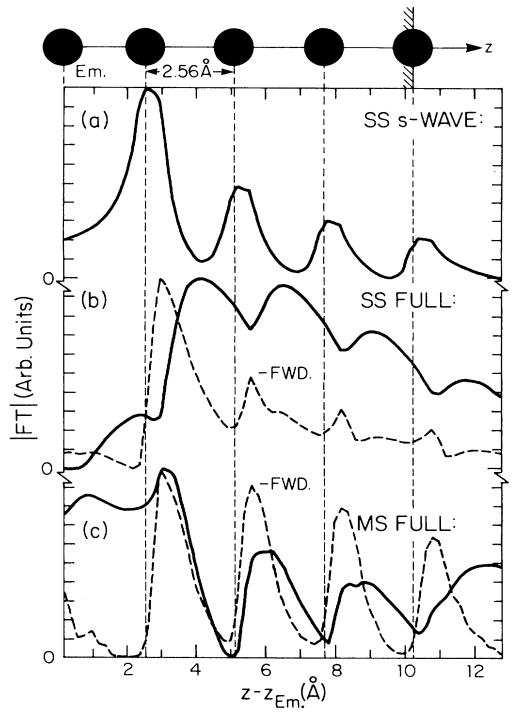

FIG. 3. Vertical line plots along the chain axis ($x=y=0.0$ Å) of the FT's for s emission from a five-atom vertical Cu chain; $\alpha=172°$. Dashed lines indicate the true atomic positions. (a) Ideal s-wave single scattering. (b) Full scattering strength in SS (solid curve) and with $\chi(\mathbf{k})$ multiplied by a forward-scattering window function with half-width of 50° (dashed curve). (c) As (b), but in MS.

partial waves); here, the peaks are significantly broadened and overlapping along the chain direction, and shifted away from their ideal positions (vertical dashed lines) and toward larger distances by amounts ranging from 0.20 to 0.43 Å. In Fig. 2(d) are results from a multiple-scattering calculation that will give rise to significant defocusing effects in emission along the chain; this is seen in the FT as a reduction of the importance of the first- and second-neighbor peaks relative to those of the more distant neighbors. In addition, however, the FT peaks in MS are better resolved than in SS and with lower background, although the positions of the peaks remain the same (shifts of 0.20–0.43 Å). Thus, MS should in one sense actually be of some benefit to holography in reducing the strong anisotropy produced by forward scattering for emitters separated by several scatterers from the detector, yielding a more s-like effective scattering amplitude. Similar results are also found for chains of two atoms (for which SS=MS [8(b),9]) and three atoms (for which the changes in going from SS to MS are much less noticeable than with five atoms).

These results also suggest that the elimination of the strong forward-scattering features from the hologram before transforming might be advantageous, and we thus show in Figs. 2(c) and 2(e) the analogous FT's for a smaller opening angle of $\alpha=120°$. There is a dramatic improvement in both the SS and MS results, with much narrower peaks and a reduction of peak shifts to 0.15–0.32 Å. Studies of adsorbate overlayers thus should benefit by not using takeoff angles that are too low, although a negative effect is that the remaining overall percentage effects in $\chi(\mathbf{k})$ will be much reduced.

In Fig. 3, we present analogous FT results for a vertical chain containing five atoms, in the form of one-dimensional plots along the chain axis. The s-wave FT in 3(a) is again well behaved and yields excellent peak posi-

tions (± 0.05–0.15 Å) and FWHM's of ~ 1.1 Å consistent with expectations for such vertical resolution. However, the full-scattering SS result [solid curve in Fig. 3(b)] shows extreme distortion, with very broad and overlapping peaks that are all significantly shifted from the true atomic positions (again vertical dashed lines) and toward larger distances by 1.4–1.7 Å. The corresponding MS results are shown by the solid curve of Fig. 3(c), and, as for the horizontal chain of Fig. 2, there is noticeable improvement in the peak widths, presumably due to defocusing. However, the peak positions are still shifted outward by amounts ranging from 0.50 to over 2.0 Å.

These aberrations could be due in part to the strong forward-focusing effects that are now directly along the axis of the hologram, and we have thus tried a smooth elimination of the forward-scattering peak from the original $\chi(\mathbf{k})$ by multiplying it by a smooth Gaussian-derived window function of the form $[1-\exp(-0.691\delta^2/\gamma^2)]$, where δ is the angular deviation of $\mathbf{k}$ from the chain axis and γ is a variable half-width of the window, here chosen from several trial values to be 50° for SS and MS. The influence of this elimination in both SS and MS is shown by the dashed curves ("$-$FWD.") in Figs. 3(b) and 3(c). There is considerable improvement in both SS and MS, with narrower peak widths and less overlap, and principal features that lie closer to the actual atomic positions (deviations of only 0.40–0.55 Å). Similar results have been obtained for chains of two and three atoms that would be appropriate for describing emitters closer to the surface.

Additional calculations that we have performed for dipole-induced S $2p$ emission into interfering s and d channels from a simulated $c(2\times 2)$S/Ni(001) overlayer indicate further that the inherent anisotropy of the outgoing waves in photoelectron diffraction can lead to even greater distortion and smearing of images, including satellite peaks, *again along forward-scattering directions.* Again we find that eliminating these strong forward peaks in $\chi(\mathbf{k})$ improves the image quality, although it is not as good as for the outgoing s-wave results discussed above.

In conclusion, electron emission holography via simple Fourier transforms and without any processing of the raw data appears capable of producing images of atomic structures at resolutions of $\sim \pm 0.3$–0.5 Å in the horizontal plane and $\sim \pm 1.0$–2.0 Å in the vertical direction. Considerable care will need to be exercised in dealing with self-interference artifacts and significant shifts and elongations of images, as well as satellite peaks, that occur preferentially along the directions of strong forward scattering. The latter effects have in fact been qualitatively observed in all of the inversions of experimental data carried out thus far [3,6]. However, the elimination of strong forward-scattering *amplitude* effects before Fourier transformation is found to significantly improve image quality as to both peak shape and position. Additional corrections for the effects of scattering *phase shifts* may lead to further improvement [3(d),5(b)]. Finally, we note a degree of redundancy in the direct-space forward-scattering peaks in $\chi(\mathbf{k})$ and the elongated images in $U(x,y;z)$, as the latter also will tend to point along dense near-neighbor directions.

This work was supported by the Office of Naval Research (Contract No. N00014-90-5-1457) and NEDO-MITI (Japan). Multiple-scattering calculations were performed at the San Diego Supercomputer Center.

[a]Present address: University of California at Davis, Davis, CA 95616, and Lawrence Berkeley Laboratory, Berkeley, CA 94720.

[1] A. Szoeke, in *Short Wavelength Coherent Radiation: Generation and Applications,* edited by D. T. Attwood and J. Boker, AIP Conference Proceedings No. 147 (American Institute of Physics, New York, 1986).

[2] (a) J. J. Barton, Phys. Rev. Lett. **61**, 1356 (1988); (b) J. Electron Spectrosc. **51**, 37 (1990).

[3] (a) H. Li and B. P. Tonner, Phys. Rev. B **40**, 10241 (1989); (b) G. K. Harp, D. K. Saldin, and B. P. Tonner, Phys. Rev. Lett. **65**, 1012 (1990); (c) Phys. Rev. B **42**, 9199 (1990); (d) B. P. Tonner, Z. L. Han, G. K. Harp, and D. K. Saldin (to be published).

[4] D. K. Saldin and P. L. de Andres, Phys. Rev. Lett. **64**, 1270 (1990).

[5] (a) C. M. Wei, T. C. Zhao, and S. Y. Tong, Phys. Rev. Lett. **65**, 2278 (1990); (b) S. Y. Tong, H. Huang, and Hua Li (to be published).

[6] G. S. Herman, S. Thevuthasan, Y. J. Kim, T. T. Tran, and C. S. Fadley (to be published).

[7] C. S. Fadley, Phys. Scr. **T17**, 39 (1987).

[8] (a) J. J Rehr and R. C. Albers, Phys. Rev. B **41**, 8139 (1990); (b) A. P. Kaduwela, G. S. Herman, D. J. Friedman, and C. S. Fadley, Phys. Scr. **41**, 948 (1990).

[9] M. L. Xu and M. Van Hove, Surf. Sci. **207**, 215 (1989).

[10] S. Y. Tong, H. C. Poon, and D. R. Snider, Phys. Rev. B **32**, 2096 (1985).